

Measurement of masses of the $\Xi_c(2645)$ and $\Xi_c(2815)$ baryons and observation of $\Xi_c(2980) \rightarrow \Xi_c(2645)\pi$

T. Lesiak,²⁷ I. Adachi,⁸ H. Aihara,⁴³ K. Arinstein,¹ A. M. Bakich,³⁸ V. Balagura,¹³ E. Barberio,²¹ I. Bedny,¹ K. Belous,¹¹ V. Bhardwaj,³³ U. Bitenc,¹⁴ S. Blyth,²⁵ A. Bozek,²⁷ M. Bračko,^{8,14,20} J. Brodzicka,⁸ T. E. Browder,⁷ Y. Chao,²⁶ A. Chen,²⁴ W. T. Chen,²⁴ B. G. Cheon,⁶ R. Chistov,¹³ I.-S. Cho,⁴⁸ S.-K. Choi,⁵ Y. Choi,³⁷ J. Dalseno,⁸ M. Dash,⁴⁷ S. Eidelman,¹ N. Gabyshev,¹ B. Golob,^{14,19} H. Ha,¹⁶ J. Haba,⁸ K. Hayasaka,²² M. Hazumi,⁸ D. Heffernan,³² Y. Hoshi,⁴¹ W.-S. Hou,²⁶ H. J. Hyun,¹⁷ K. Inami,²² A. Ishikawa,³⁴ H. Ishino,⁴⁴ R. Itoh,⁸ M. Iwasaki,⁴³ Y. Iwasaki,⁸ N. J. Joshi,³⁹ D. H. Kah,¹⁷ H. Kaji,²² J. H. Kang,⁴⁸ H. Kawai,² T. Kawasaki,²⁹ H. Kichimi,⁸ H. J. Kim,¹⁷ S. K. Kim,³⁶ Y. J. Kim,⁴ S. Korpar,^{14,20} P. Križan,^{14,19} P. Krokovny,⁸ C. C. Kuo,²⁴ Y.-J. Kwon,⁴⁸ S. Lange,³ J. S. Lee,³⁷ M. J. Lee,³⁶ S. E. Lee,³⁶ J. Li,⁷ S.-W. Lin,²⁶ C. Liu,³⁵ D. Liventsev,¹³ F. Mandl,¹² S. McOnie,³⁸ T. Medvedeva,¹³ K. Miyabayashi,²³ H. Miyake,³² H. Miyata,²⁹ Y. Miyazaki,²² R. Mizuk,⁴⁹ G. R. Moloney,²¹ Y. Nagasaka,⁹ M. Nakao,⁸ Z. Natkaniec,²⁷ S. Nishida,⁸ O. Nitoh,⁴⁶ T. Nozaki,⁸ S. Ogawa,⁴⁰ T. Ohshima,²² S. Okuno,¹⁵ H. Ozaki,⁸ G. Pakhlova,¹³ H. Palka,²⁷ H. K. Park,¹⁷ L. S. Peak,³⁸ R. Pestotnik,¹⁴ L. E. Pilonen,⁴⁷ H. Sahoo,⁷ Y. Sakai,⁸ O. Schneider,¹⁸ K. Senyo,²² M. E. Sevior,²¹ M. Shapkin,¹¹ H. Shibuya,⁴⁰ J.-G. Shiu,²⁶ B. Shwartz,¹ A. Sokolov,¹¹ S. Stanič,³⁰ M. Starič,¹⁴ T. Sumiyoshi,⁴⁵ F. Takasaki,⁸ M. Tanaka,⁸ G. N. Taylor,²¹ Y. Teramoto,³¹ I. Tikhomirov,¹³ K. Trabelsi,⁸ T. Tsuboyama,⁸ S. Uehara,⁸ K. Ueno,²⁶ T. Uglov,¹³ Y. Unno,⁶ S. Uno,⁸ P. Urquijo,²¹ G. Varner,⁷ K. E. Varvell,³⁸ K. Vervink,¹⁸ C. C. Wang,²⁶ C. H. Wang,²⁵ M.-Z. Wang,²⁶ P. Wang,¹⁰ X. L. Wang,¹⁰ Y. Watanabe,¹⁵ R. Wedd,²¹ E. Won,¹⁶ B. D. Yabsley,³⁸ H. Yamamoto,⁴² Y. Yamashita,²⁸ M. Yamauchi,⁸ Z. P. Zhang,³⁵ V. Zhilich,⁵⁰ V. Zhulanov,¹ A. Zupanc,¹⁴ and O. Zyukova¹

(The Belle Collaboration)

¹*Budker Institute of Nuclear Physics, Novosibirsk, Russia*

²*Chiba University, Chiba, Japan*

³*Justus-Liebig-Universität Gießen, Gießen, Germany*

⁴*The Graduate University for Advanced Studies, Hayama, Japan*

⁵*Gyeongsang National University, Chinju, South Korea*

⁶*Hanyang University, Seoul, South Korea*

⁷*University of Hawaii, Honolulu, HI, USA*

⁸*High Energy Accelerator Research Organization (KEK), Tsukuba, Japan*

⁹*Hiroshima Institute of Technology, Hiroshima, Japan*

¹⁰*Institute of High Energy Physics,*

Chinese Academy of Sciences, Beijing, PR China

¹¹*Institute for High Energy Physics, Protvino, Russia*

¹²*Institute of High Energy Physics, Vienna, Austria*

¹³*Institute for Theoretical and Experimental Physics, Moscow, Russia*

¹⁴*J. Stefan Institute, Ljubljana, Slovenia*

¹⁵*Kanagawa University, Yokohama, Japan*

- ¹⁶*Korea University, Seoul, South Korea*
¹⁷*Kyungpook National University, Taegu, South Korea*
¹⁸*École Polytechnique Fédérale de Lausanne, EPFL, Lausanne, Switzerland*
¹⁹*Faculty of Mathematics and Physics,
University of Ljubljana, Ljubljana, Slovenia*
²⁰*University of Maribor, Maribor, Slovenia*
²¹*University of Melbourne, Victoria, Australia*
²²*Nagoya University, Nagoya, Japan*
²³*Nara Women's University, Nara, Japan*
²⁴*National Central University, Chung-li, Taiwan*
²⁵*National United University, Miao Li, Taiwan*
²⁶*Department of Physics, National Taiwan University, Taipei, Taiwan*
²⁷*H. Niewodniczanski Institute of Nuclear Physics, Krakow, Poland*
²⁸*Nippon Dental University, Niigata, Japan*
²⁹*Niigata University, Niigata, Japan*
³⁰*University of Nova Gorica, Nova Gorica, Slovenia*
³¹*Osaka City University, Osaka, Japan*
³²*Osaka University, Osaka, Japan*
³³*Panjab University, Chandigarh, India*
³⁴*Saga University, Saga, Japan*
³⁵*University of Science and Technology of China, Hefei, PR China*
³⁶*Seoul National University, Seoul, South Korea*
³⁷*Sungkyunkwan University, Suwon, South Korea*
³⁸*University of Sydney, Sydney, NSW, Australia*
³⁹*Tata Institute of Fundamental Research, Mumbai, India*
⁴⁰*Toho University, Funabashi, Japan*
⁴¹*Tohoku Gakuin University, Tagajo, Japan*
⁴²*Tohoku University, Sendai, Japan*
⁴³*Department of Physics, University of Tokyo, Tokyo, Japan*
⁴⁴*Tokyo Institute of Technology, Tokyo, Japan*
⁴⁵*Tokyo Metropolitan University, Tokyo, Japan*
⁴⁶*Tokyo University of Agriculture and Technology, Tokyo, Japan*
⁴⁷*Virginia Polytechnic Institute and State University, Blacksburg, VA, USA*
⁴⁸*Yonsei University, Seoul, South Korea*
⁴⁹*Institute for Theoretical and Experimental Physics, Moscow*
⁵⁰*Budker Institute of Nuclear Physics, Novosibirsk*

Abstract

We report a precise measurement of the masses of the $\Xi_c(2645)$ and $\Xi_c(2815)$ baryons using a data sample of 414 fb^{-1} collected by the Belle collaboration at the KEKB e^+e^- collider. The states $\Xi_c(2645)^{0,+}$ are observed in the $\Xi_c^{+,0}\pi^{-,+}$ decay modes, while the $\Xi_c(2815)^{0,+}$ are reconstructed in the $\Xi_c(2645)^{+,0}\pi^{-,+}$ decay modes. The following mass splittings are determined: $m_{\Xi_c(2645)^+} - m_{\Xi_c(2645)^0} = (-0.1 \pm 0.3(\text{stat}) \pm 0.6(\text{syst})) \text{ MeV}/c^2$ and $m_{\Xi_c(2815)^+} - m_{\Xi_c(2815)^0} = (-3.4 \pm 1.9(\text{stat}) \pm 0.9(\text{syst})) \text{ MeV}/c^2$ with a much better precision than the current world averages. We also observe a new decay mode, $\Xi_c(2980)^{0,+} \rightarrow \Xi_c(2645)^{+,0}\pi^{-,+}$.

PACS numbers: 14.40.Lb, 13.25.Ft, 13.25.Gv, 13.20.Jf

INTRODUCTION

The study of charmed baryons has recently been a focus of significant experimental effort [1, 2, 3, 4, 5, 6, 7, 8]. Several new excited states, such as the $\Xi_c(2980)$, $\Xi_c(3055)$, $\Xi_c(3077)$, $\Xi_c(3123)$ and $\Lambda_c(2940)$ have been observed, or their properties determined for the first time, enabling tests of quark (and other) models and predictions of heavy quark symmetry [9, 10].

This paper presents a study of exclusive decays of the $\Xi_c(2645)^0$, $\Xi_c(2645)^+$, $\Xi_c(2815)^0$ and $\Xi_c(2815)^+$ baryons [11] and a determination of their masses and the corresponding mass splittings within isospin doublets. The $\Xi_c(2645)^0$ and $\Xi_c(2645)^+$ are reconstructed in the $\Xi_c^+\pi^-$ and $\Xi_c^0\pi^+$ decay modes, respectively. The latter mode was first observed by the CLEO collaboration [12], while the former decay mode is observed here for the first time. For the hyperons $\Xi_c(2815)^0$ and $\Xi_c(2815)^+$, first seen by the CLEO collaboration [13], the decays into $\Xi_c(2645)^+\pi^-$ and $\Xi_c(2645)^0\pi^+$ are observed.

In the mass spectra of $\Xi_c(2645)^{+,0}\pi^{-,+}$ pairs, we observe clear peaks close to the $\Xi_c(2980)^{0,+}$ reported by the Belle [1] and BaBar [2] collaborations in the $\Lambda_c^+K^-\pi^+$ and $\Lambda_c^+K_S^0\pi^-$ final states.

This article is organized as follows. In the first two sections we describe the data sample and the reconstruction of Ξ_c baryons. The next two sections are devoted to the precise determination of the $\Xi_c(2645)$ and $\Xi_c(2815)$ masses. Finally, in the last section, we discuss the mass peaks observed above the $\Xi_c(2815)^{+,0}$ states in the $\Xi_c(2645)^{0,+}\pi^{+,-}$ systems.

DETECTOR AND DATA SAMPLE

The data used for this study were collected on the $\Upsilon(4S)$ resonance using the Belle detector at the KEKB asymmetric-energy e^+e^- collider [14]. The integrated luminosity of the data sample is 414 fb^{-1} .

The Belle detector is a large-solid-angle magnetic spectrometer that consists of a silicon vertex detector (SVD), a 50-layer central drift chamber (CDC), an array of aerogel threshold Cherenkov counters (ACC), a barrel-like arrangement of time-of-flight scintillation counters (TOF), and an electromagnetic calorimeter comprised of CsI(Tl) crystals (ECL) located inside a superconducting solenoid coil that provides a 1.5 T magnetic field. An iron flux-return located outside of the coil is instrumented to detect K_L^0 mesons and to identify muons (KLM). A detailed description of the Belle detector can be found elsewhere [15].

RECONSTRUCTION

Reconstruction of Ξ_c , $\Xi_c(2645)$ and $\Xi_c(2815)$ decays for this analysis proceeds in three steps: reconstruction of tracks and their identification as protons, kaons or pions; combination of tracks to reconstruct Λ and Ξ^- hyperons; and the selection of Ξ_c candidates from combinations of tracks and hyperons. The method used for each step is described in the following sections.

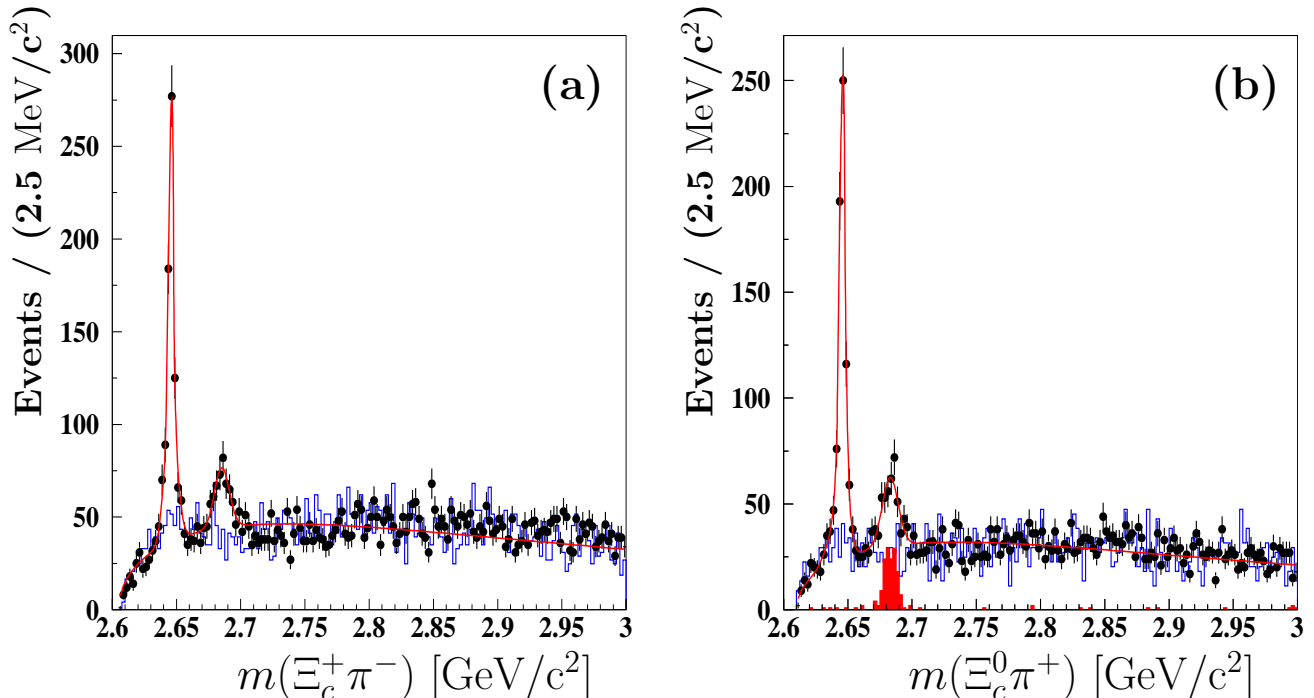


FIG. 1: Invariant mass distributions for (a) $\Xi_c^+\pi^-$ ($\Xi_c^+ \rightarrow \Xi^- \pi^+ \pi^+$) and (b) $\Xi_c^0\pi^+$ ($\Xi_c^0 \rightarrow \Xi^- \pi^+$). Curves correspond to the fit described in the text. The histograms show the Ξ_c mass sidebands. The second peak is due to the feed-down from $\Xi_c(2790) \rightarrow \Xi_c'(2579)\pi, \Xi_c' \rightarrow \Xi_c\gamma$, as determined from Monte Carlo simulations and marked in (b) as a shaded histogram.

Track reconstruction and identification

Charged tracks are reconstructed from hits in the CDC using a Kalman filter [16] and matched to hits in the SVD. Quality criteria are then applied. All tracks other than those used to form Λ and Ξ^- candidates, are required to have impact parameters relative to the interaction point (IP) of less than 0.5 cm in the $r - \phi$ plane, and 5 cm in the z direction [17]. The transverse momentum of each track is required to exceed 0.1 GeV/c, in order to reduce the low momentum combinatorial background.

Hadron identification is based on information from the CDC (energy loss dE/dx), TOF and ACC, combined to form likelihoods $\mathcal{L}(p)$, $\mathcal{L}(K)$ and $\mathcal{L}(\pi)$ for the proton, kaon and pion hypotheses, respectively. These likelihoods are combined to form ratios $\mathcal{P}(K/\pi) = \mathcal{L}(K)/(\mathcal{L}(K) + \mathcal{L}(\pi))$ and $\mathcal{P}(p/K) = \mathcal{L}(p)/(\mathcal{L}(p) + \mathcal{L}(K))$, spanning the range from zero to one, which are then used to identify individual tracks [15]. Pion candidates, except those coming from the decay of the Λ hyperon, should satisfy both a proton and a kaon veto: $\mathcal{P}(p/K) < 0.98$ and $\mathcal{P}(K/\pi) < 0.98$.

Electrons are identified using a similar likelihood ratio $\mathcal{P}_e = \mathcal{L}_e/(\mathcal{L}_e + \mathcal{L}_{\text{non-}e})$, based on a combination of dE/dx measurements in the CDC, the response of the ACC, E/p , where p is the momentum of the track and E the energy of the associated cluster in the ECL, as well as matching between the track and the ECL cluster position and the transverse shower shape. All tracks with $\mathcal{P}_e > 0.98$ are assumed to be electrons, and removed from the proton, kaon and pion samples.

Reconstruction of Λ and Ξ^-

We reconstruct Λ hyperons in the $\Lambda \rightarrow p\pi^-$ decay mode, requiring the proton track to satisfy $\mathcal{P}(p/K) > 0.1$ [18], and fitting the p and π tracks to a common vertex. To reduce the number of poorly reconstructed candidates, the $\chi^2/n.d.f.$ [19] of the vertex should not exceed 25 (removing approximately 2% of signal candidates) and the difference in the z -coordinate between the proton and pion at the vertex is required to be less than 2 cm. Due to the large $c\tau$ factor for Λ hyperons (7.89 cm), we demand that the distance between the decay vertex and the IP in the $r - \phi$ plane be greater than 1 cm. The invariant mass of the proton-pion pair is required to be within 2.4 MeV/c² (≈ 2.5 standard deviations) of the nominal Λ mass. The mean value of the Λ signal in the reconstructed mass distribution is found to be 1115.7 ± 0.1 MeV/c², in agreement with the world average value [20].

We reconstruct Ξ^- hyperons in the decay mode $\Xi^- \rightarrow \Lambda\pi^-$. The Λ and π candidates are fitted to a common vertex, for which we require $\chi^2/n.d.f. < 25$ (removing approximately 2% of signal candidates). The distance between the Ξ^- decay vertex position and the IP in the $r - \phi$ plane should be at least 5 mm, and less than the corresponding distance between the IP and the Λ vertex. The invariant mass of the $\Lambda\pi^-$ pair is required to be within 7.5 MeV/c² of the nominal value (≈ 2.5 standard deviations). The mass of the Ξ^- is found to be 1321.78 ± 0.21 MeV/c², in agreement with the PDG average: 1321.34 ± 0.14 MeV/c² [20].

Reconstruction of Ξ_c , $\Xi_c(2645)$ and $\Xi_c(2815)$

The reconstructed Λ and Ξ^- candidates and the remaining charged hadrons in an event are combined to form candidates for the decays $\Xi_c^+ \rightarrow \Xi^- \pi^+ \pi^+$ and $\Xi_c^0 \rightarrow \Xi^- \pi^+$. The signal region is defined by the reconstructed mass windows (2.455–2.485) GeV/c² for the former, and (2.45–2.49) GeV/c² for the latter decay. All particles forming the Ξ_c candidate are then fitted to a common vertex constraining their invariant mass to the average PDG values [20]. A goodness-of-fit criterion is applied: $\chi^2/n.d.f. < 50$ (removing approximately 5% of signal candidates).

The decays $\Xi_c(2645)^0 \rightarrow \Xi_c^+ \pi^-$ and $\Xi_c(2645)^+ \rightarrow \Xi_c^0 \pi^+$ are reconstructed by fitting pairs of charged pions and Ξ_c candidates to a common vertex. The combinations are accepted if they satisfy the criterion $\chi^2/n.d.f. < 10$ (removing approximately 10% of signal candidates) and if the momentum of the $\Xi_c\pi$ system in the center-of-mass system (CMS) exceeds 2.5 GeV/c. Due to the hard momentum spectrum of baryons produced in e^+e^- processes, this requirement significantly suppresses the combinatorial background.

Figure 1 shows a clear $\Xi_c(2645)$ signal in $\Xi_c^+ \pi^-$ and $\Xi_c^0 \pi^+$ mass distributions. The second less pronounced maximum above the $\Xi_c(2645)$ peak is found to be a feed-down of the decay $\Xi_c(2790) \rightarrow \Xi_c'(2579)\pi$, $\Xi_c' \rightarrow \Xi_c\gamma$ (first observed by the CLEO collaboration [21]). When the photon is missed, the $\Xi_c\pi$ invariant mass peaks around 2.68 GeV/c². Both mass and width of the feed-down are in agreement with Monte Carlo (MC) expectations.

The decays $\Xi_c(2815)^0 \rightarrow \Xi_c(2645)^+ \pi^-$ and $\Xi_c(2815)^+ \rightarrow \Xi_c(2645)^0 \pi^+$ are reconstructed by fitting the $\Xi_c(2645)$ candidates and an additional charged pion to a common vertex. Combinations are accepted if they satisfy the criterion $\chi^2/n.d.f. < 10$ (removing approximately 10% of signal candidates), and if the momentum of the $\Xi_c(2645)\pi$ system in the CMS exceeds 2.5 GeV/c. The signal region for the $\Xi_c(2645)$ is defined as (2.635–2.655) GeV/c² (≈ 2.5 standard deviations) for both decay chains. Figure 2 shows a clear signal of the $\Xi_c(2815)$ baryon in the $\Xi_c(2645)^0 \pi^+$ and $\Xi_c(2645)^+ \pi^-$ mass distributions. Here, we also

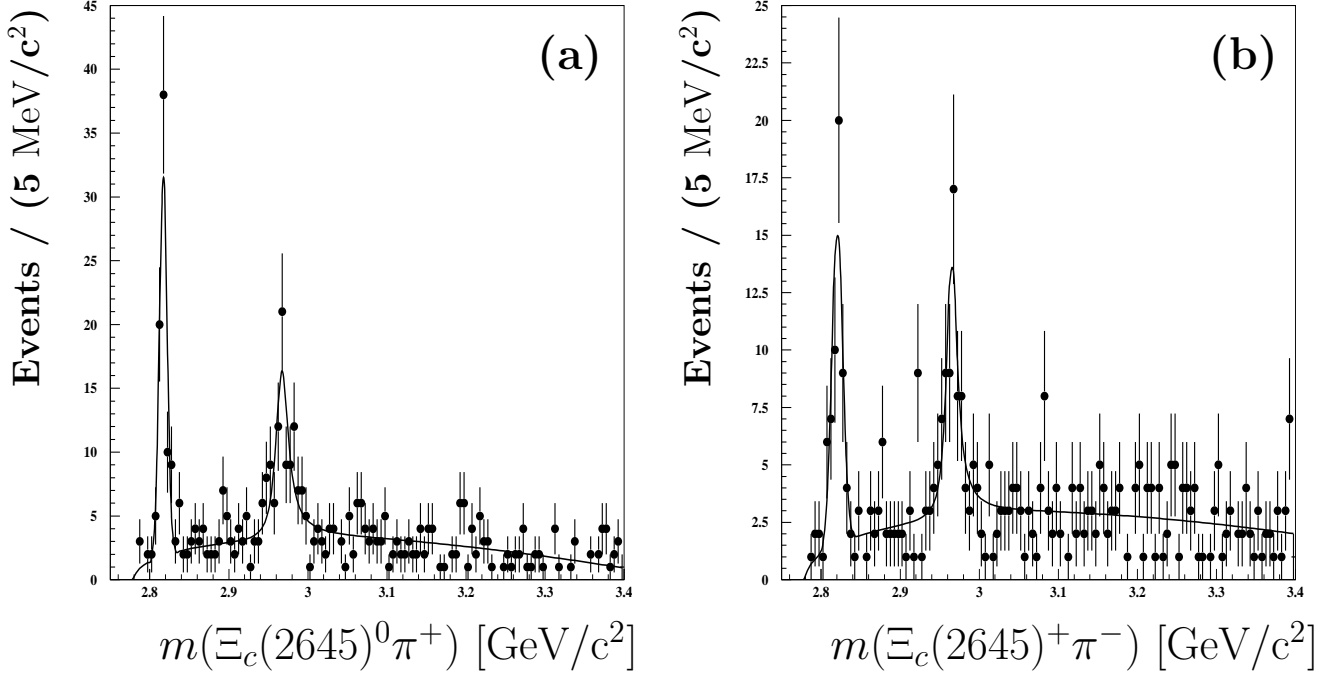


FIG. 2: Invariant mass distribution for **(a)** $\Xi_c(2645)^0\pi^+$ ($\Xi_c(2645)^0 \rightarrow \Xi_c^+\pi^-$, $\Xi_c^+ \rightarrow \Xi^-\pi^+\pi^+$) and **(b)** $\Xi_c(2645)^+\pi^-$ ($\Xi_c(2645)^+ \rightarrow \Xi_c^0\pi^+$, $\Xi_c^0 \rightarrow \Xi^-\pi^+$). Curves correspond to the fit described in the text.

find a broader peak near $2.98 \text{ GeV}/c^2$ in the two charge states.

$\Xi_c(2645)$ MASS DETERMINATION

We extract the signal yield and the $\Xi_c(2645)^{+,0}$ mass and width from a fit to the invariant mass distribution of $\Xi_c^{0,+}\pi^{+,-}$ pairs, respectively. We use two Gaussians with a common mean for the signal of the $\Xi_c(2645)$:

$$\mathcal{P}_s(m; \mu, \sigma_1, \sigma_2, f_1) = f_1 \mathcal{G}(m; \mu, \sigma_1) + (1 - f_1) \mathcal{G}(m; \mu, \sigma_2), \quad (1)$$

(where the parameter f_1 denotes a fractional yield of the first Gaussian) and a single Gaussian $\mathcal{G}_f(m; \mu_f, \sigma_f)$ for the feed-down due to the $\Xi_c(2790)$:

$$\mathcal{P}_f(m; \mu_f, \sigma_f) = \mathcal{G}(m; \mu_f, \sigma_f). \quad (2)$$

The background is described by a threshold function ($\sqrt{m - m_0}$, where m_0 corresponds to the threshold mass value) multiplied by a fourth-order polynomial p_4 with coefficients $c_i, i = 0, 1, \dots, 4$:

$$\mathcal{P}_b(m; m_0, c_0, c_1, c_2, c_3, c_4) = \sqrt{m - m_0} \cdot p_4. \quad (3)$$

An additional contribution is due to the reflections from the decay chains $\Xi_c(2815)^{+,0} \rightarrow \Xi_c(2645)^{0,+}\pi^{+,-}$, $\Xi_c(2645)^{0,+} \rightarrow \Xi_c^{0,+}\pi^0$, where the neutral pion remains undetected, close to the mass peak of the $\Xi_c(2645)$. The shape of this reflection in $\Xi_c^0\pi^+$ pairs is taken into account by fitting the mass spectra of $\Xi_c^+\pi^+$ in the $\Xi_c(2815)^+ \rightarrow \Xi_c(2645)^0\pi^+ \rightarrow (\Xi_c^+\pi^-)\pi^+$ decay chain. Similarly, for the right-sign combinations $\Xi_c^+\pi^-$, the invariant mass of the

TABLE I: Signal yields and $\Xi_c(2645)$ masses and widths, obtained from the fits to the $\Xi_c\pi$ mass spectra. f_1 denotes the fraction of the first (narrower) Gaussian; σ_1 and σ_2 are the Gaussian widths. Errors shown for signal yields, f_1 , σ_1 and σ_2 are statistical only.

Particle	# of events	Mass [MeV/c ²]	f_1	σ_1 [MeV]	σ_2 [MeV]	$\chi^2/n.d.f.$
$\Xi_c(2645)^0$	611 ± 32	$2645.7 \pm 0.2_{-0.7}^{+0.6}$	0.44 ± 0.10	1.5 ± 0.3	4.7 ± 0.6	1.69
$\Xi_c(2645)^+$	578 ± 32	$2645.6 \pm 0.2_{-0.8}^{+0.6}$	0.59 ± 0.11	1.9 ± 0.3	5.5 ± 1.1	1.16

wrong-sign pairs $\Xi_c^0\pi^-$ from the decay chain $\Xi_c(2815)^0 \rightarrow \Xi_c(2645)^+\pi^- \rightarrow (\Xi_c^0\pi^+)\pi^-$ is used. The reflection peak is parameterized by a single Gaussian:

$$\mathcal{P}_r(m; \mu_r, \sigma_r) = \mathcal{G}(m; \mu_r, \sigma_r). \quad (4)$$

Thus the overall fit parameterization reads

$$\mathcal{P} = c_s\mathcal{P}_s + c_f\mathcal{P}_f + c_b\mathcal{P}_b + c_r\mathcal{P}_r, \quad (5)$$

where the yields c_s , c_f and c_b are to be determined from the fit. The yields of the peaks due to the reflections (c_r) are estimated according to the formulae

$$c_r = N(\Xi_c(2815)^0) \times \frac{1}{2} \times \frac{\epsilon(\Xi_c^+)}{\epsilon(\Xi_c^0\pi^+)} \quad (6)$$

and

$$c_r = N(\Xi_c(2815)^+) \times \frac{1}{2} \times \frac{\epsilon(\Xi_c^0)}{\epsilon(\Xi_c^+\pi^-)} \quad (7)$$

for $\Xi_c^+\pi^-$ ($\Xi_c^0\pi^+$) pairs, respectively [22]. Here the values of $N(\Xi_c(2815)^{0,+})$ are taken from Table III (the results of the fit to the $\Xi_c(2645)\pi$ mass distribution, described below), $1/2$ is the isospin factor weight of $\Xi_c(2645)$ decays, with a π^0 , to those involving a π^\pm . The efficiencies $\epsilon(\Xi_c^+) = 4.55 \pm 0.07\%$ ($\epsilon(\Xi_c^0) = 7.13 \pm 0.14\%$) correspond to the exclusive decays $\Xi_c^+ \rightarrow \Xi^- \pi^+ \pi^+$ ($\Xi_c^0 \rightarrow \Xi^- \pi^+$), respectively. They are estimated in our previous measurement (see Table 1 of [8]). Other parameters determined by the fit are μ , σ_1 , σ_2 , f_1 , μ_f and σ_f .

The shape of the background function is fixed from the fit to the spectrum of $\Xi_c\pi$ invariant masses using the Ξ_c candidates mass sideband: (2.37–2.41) GeV/c² and (2.52–2.57) GeV/c². Results of the fits are summarized in Table I.

As a cross-check, the same selection criteria as described above are also applied to MC samples: $e^+e^- \rightarrow c\bar{c}$ and $e^+e^- \rightarrow q\bar{q}$, $q = u, d, s$ with no signal decays included. The background shapes in the $\Xi_c\pi$ mass spectra for data and MC are in good agreement. The mass of each $\Xi_c(2645)$ state is obtained from a signal MC sample in which one Ξ_c decay occurs per event: both are found to be within 0.2 MeV/c² of the generated value.

The systematic uncertainty on the $\Xi_c(2645)$ mass determination is evaluated as follows (Table II). First, we consider systematic uncertainties related to the fit procedure. To take into account imperfect understanding of the signal resolution, we perform fits varying the signal widths by their statistical errors, and compare with values where the widths are floated: the mass changes by 0.1 MeV/c². For each mode we modify the mass range covered by the fit (extending it by 20%), the bin width (2.5–1.0 MeV/c²) and the parameterization of the

TABLE II: Systematic uncertainties on the mass determination of the $\Xi_c(2645)$ and $\Xi_c(2815)$.

Source	Systematic error [MeV/c ²]			
	$\Xi_c(2645)^0$	$\Xi_c(2645)^+$	$\Xi_c(2815)^+$	$\Xi_c(2815)^0$
(1) Signal width	0.1	0.1	0.3	0.5
(2) Fit range	0.0	0.0	0.1	0.0
(3) Bin width	0.1	0.0	0.1	0.4
(4) Background parameterization	0.1	0.0	0.0	0.2
(5) Decay length of the $\Xi^-(\Lambda)$	+0.24 -0.30	+0.24 -0.30	+0.24 -0.30	+0.24 -0.30
(6) Momentum of the $\Xi^-(\Lambda)$	+0.25 -0.27	+0.24 -0.30	+0.25 -0.27	+0.24 -0.30
(7) Comparison to [4]	-0.28	-0.28	-0.28	-0.28
(8) Azimuthal angle dependence	+0.17 -0.19	+0.17 -0.19	+0.17 -0.19	+0.17 -0.19
(9) CMS momentum $p^*(\Xi_c(2645))$ dependence	0.09	0.09	0.09	0.09
(10) Reflection from the $\Xi_c(2815)$	+0.1 -0.2	+0.1 -0.2	n.a.	n.a.
(11) Mass-constrained fit of the Ξ_c	0.4	0.4	0.4	0.4
Total systematic error	+0.6 -0.7	+0.6 -0.8	+0.7 -0.8	+0.9 -1.0

background (by varying values of parameters obtained from the Ξ_c sidebands by $\pm 1 \sigma$). The resulting changes in the fitted masses are at most 0.1 MeV/c², depending on the decay.

To estimate the possible dependence of the $\Xi_c(2645)$ mass on the momentum and decay length of the Ξ^- and Λ hyperons we study the decay $\Lambda_c \rightarrow \Xi^- K^+ \pi^+$. A fit to the $\Xi K \pi$ invariant mass distribution yields $m(\Lambda_c) = 2286.63 \pm 0.09$ MeV/c² (statistical error only). The Λ_c mass is also determined in bins of the momentum and decay length of the hyperon Ξ , which leads to systematic uncertainties of $_{-0.27}^{+0.25}$ MeV/c² and $_{-0.30}^{+0.24}$ MeV/c², respectively.

To test the modeling of the detector response (alignment, uniformity of magnetic field, correct treatment of specific ionization and scattering in the material), which could cause a bias in the overall mass scale, we study $\Lambda_c^+ \rightarrow p K \pi$ decays. A fit to the $p K \pi$ invariant mass distribution yields $m(\Lambda_c) = 2286.74 \pm 0.02$ MeV/c² (statistical error only). The above value is compared to the recent measurement by the BaBar collaboration [4], which yields $m(\Lambda_c) = 2286.46 \pm 0.14$ MeV/c². As a result, a -0.28 MeV/c² shift is assigned as a systematic error. The mass of the Λ_c reconstructed in $p K \pi$ is also determined in bins of the azimuthal angle. The maximal deviations with respect to the value given above are assigned as the corresponding systematic errors, yielding $_{-0.19}^{+0.17}$ MeV/c². The same study, performed in bins of Λ_c center-of-mass momentum provides an estimate of ± 0.09 MeV/c² as the respective systematic uncertainty.

The uncertainty on the parameters of the reflection due to the decays of $\Xi_c(2815)$ results in a systematic error of $_{-0.2}^{+0.1}$ MeV/c² estimated by performing the fit with the removal of the reflection contribution and also by varying its width and yield within their statistical errors.

The $\Xi_c(2645)$ mass also depends on the value of $m(\Xi_c)$ applied in the mass-constrained fit. A change of $m(\Xi_c)$ almost linearly transforms to a shift in the measured value of $m(\Xi_c(2645))$. As a result, we include a systematic uncertainty equal to the statistical error in the determination of the Ξ_c mass [20], i.e. ± 0.4 MeV/c² both for the Ξ_c^+ and Ξ_c^0 .

It is also checked that the measured mass value is stable within one standard deviation while fitting separately the spectra corresponding to particles and antiparticles in the final

state. The total systematic uncertainty is obtained by adding the individual contributions in quadrature.

The masses of the $\Xi_c(2645)^+$ and $\Xi_c(2645)^0$ (Table I) are in agreement with, and more accurate than the current PDG averages [20]. Assuming that uncertainties (5)–(10) from Table II are the same for charged and neutral $\Xi_c(2645)$'s and, as such, cancel in the $\Xi_c(2645)^+ - \Xi_c(2645)^0$ mass splitting, we find the mass difference between the charged and neutral states to be:

$$m_{\Xi_c(2645)^+} - m_{\Xi_c(2645)^0} = (-0.1 \pm 0.3(\text{stat}) \pm 0.6(\text{syst})) \text{ MeV}/c^2. \quad (8)$$

$\Xi_c(2815)$ MASS DETERMINATION

For each decay mode, we extract the signal yield and the $\Xi_c(2815)$ mass and width from a fit to the invariant mass distribution of $\Xi_c(2645)\pi$ pairs. We use a single Gaussian for the signal from the $\Xi_c(2815)$ and a Breit-Wigner shape convoluted with a Gaussian for the peak near $m(\Xi_c(2645)\pi) = 2980 \text{ MeV}/c^2$ (we denote this peak as $\Xi_c(2980)$). The width of the latter Gaussian, describing the experimental mass resolution, is fixed from the MC simulation to the value of $2.2 \pm 0.2 \text{ MeV}$. The background is parameterized by a threshold function multiplied by a first-order polynomial with coefficients d_0 and d_1 :

$$\mathcal{P}_b(m; m_0, d_0, d_1) = \text{atan}(\sqrt{m - m_0}) \times p_1. \quad (9)$$

The fit results are summarized in Tables III and IV for the $\Xi_c(2815)$ and $\Xi_c(2980)$ signals, respectively.

TABLE III: Signal yields and $\Xi_c(2815)$ masses and widths, obtained from the fits to the $\Xi_c(2645)\pi$ mass spectra.

Particle	# of events	Mass [MeV/ c^2]	Gaussian width [MeV]	$\chi^2/n.d.f.$
$\Xi_c(2815)^+$	72.5 ± 9.6	$2817.0 \pm 1.2(\text{stat})_{-0.8}^{+0.7}(\text{syst})$	4.9 ± 0.9	1.03
$\Xi_c(2815)^0$	47.5 ± 7.8	$2820.4 \pm 1.4(\text{stat})_{-1.0}^{+0.9}(\text{syst})$	6.9 ± 1.1	0.97

TABLE IV: Signal yields and $\Xi_c(2980)$ masses and natural widths, obtained from the fits to the $\Xi_c(2645)\pi$ mass spectra.

Particle	# of events	Mass [MeV/ c^2]	Γ , natural width [MeV]	Significance [σ]
$\Xi_c(2980)^+$	78.3 ± 13.4	$2967.7 \pm 2.3(\text{stat})_{-1.2}^{+1.1}(\text{syst})$	$18 \pm 6 \pm 3$	7.3
$\Xi_c(2980)^0$	56.9 ± 12.5	$2965.7 \pm 2.4(\text{stat})_{-1.2}^{+1.1}(\text{syst})$	$15 \pm 6 \pm 3$	6.1

The systematic uncertainties on the $\Xi_c(2815)$ mass determination are estimated following the procedure used for the $\Xi_c(2645)$. The total systematic uncertainty is obtained by adding the individual contributions in quadrature (Table II).

The masses of the $\Xi_c(2815)^+$ and $\Xi_c(2815)^0$ (Table III) are in agreement with the CLEO [13] measurements. For the charged state the accuracy is comparable to [13], while for the neutral one it is better. Assuming that uncertainties (5)–(9) from Table II are the same for charged and neutral $\Xi_c(2815)$ and as such cancel in the $\Xi_c(2815)^+ - \Xi_c(2815)^0$ mass splitting, we find the mass difference between the charged and neutral states to be

$$m_{\Xi_c(2815)^+} - m_{\Xi_c(2815)^0} = (-3.4 \pm 1.9(\text{stat}) \pm 0.9(\text{syst})) \text{ MeV}/c^2. \quad (10)$$

OBSERVATION OF $\Xi_c(2980) \rightarrow \Xi_c(2645)\pi$

The mass of the $\Xi_c(2980)^0$ (Table IV) is compatible with the masses of the $\Xi_c(2980)^0$, decaying to $\Lambda_c^+ K_s^0 \pi^-$, as observed by Belle [1] and confirmed by BaBar [2]. The width of the $\Xi_c(2980)^0$ is smaller, but statistically consistent with the value measured by BaBar: $(31 \pm 7 \pm 8)$ MeV.

For the charged state $\Xi_c(2980)^+$, the mass given in Table IV is in agreement with the value determined by BaBar $((2969.3 \pm 2.2 \pm 1.7)$ MeV/ c^2) and smaller than the result in our observation of $\Xi_c(2980) \rightarrow \Lambda_c^+ K^- \pi^+$ $(2978.5 \pm 2.1 \pm 2.0)$ MeV/ c^2 . The fitted width of the $\Xi_c(2980)^+$ is smaller than the value found by Belle $(43.5 \pm 7.5 \pm 7.0)$ MeV and BaBar $(27 \pm 8 \pm 2)$ MeV. To estimate the significance of the $\Xi_c(2980)^{+,0}$ observation, the fit is repeated omitting the signal component due to this state from the fit. The significance is determined from $-2 \ln(\mathcal{L}_0/\mathcal{L})$, where \mathcal{L} and \mathcal{L}_0 refer to the maximum of the default likelihood function (describing also the $\Xi_c(2980)$) and the likelihood function omitting this signal component, respectively. This quantity should be distributed as χ^2 ($n.d.f. = 3$), as three parameters are free for the signal.

The systematic uncertainties on the $\Xi_c(2980)$ mass are determined following the procedure used for the $\Xi_c(2645)$ and $\Xi_c(2815)$. The uncertainty due to the fit procedure is determined to be ± 0.9 MeV/ c^2 by varying the bin width and the experimental resolution within its error (2.2 ± 0.2) MeV and by fitting the background with a second-order polynomial. The above mentioned procedures of varying the bin width and the experimental resolution within its error are also used to determine the systematic uncertainty of the natural width of the $\Xi_c(2980)$ (Table IV). The total systematic uncertainty on the $\Xi_c(2980)$ mass determination (Table IV) is obtained by adding in quadrature the uncertainty due to the fit procedure and the contributions (5–9) and (11), as given in Table II.

Given the uncertainties in the measured masses and widths of the $\Xi_c(2980)$, this state is consistent with the charmed baryon observed in $\Lambda_c K \pi$ final state, the $\Xi_c(2980)$. No signals are observed in the $\Xi_c(2645)\pi$ mass spectra near the masses of 3055, 3077 and 3123 MeV/ c^2 , corresponding to the new states observed by Belle [1] and BaBar [2] in $\Lambda_c K \pi$ decays.

CONCLUSIONS

Based on a large sample of the Ξ_c hyperons, the masses of $\Xi_c(2645)$ and $\Xi_c(2815)$ baryons are measured (Table V) together with the mass splittings within isospin doublets:

$$m_{\Xi_c(2645)^+} - m_{\Xi_c(2645)^0} = (-0.1 \pm 0.3(\text{stat}) \pm 0.6(\text{syst})) \text{ MeV}/c^2,$$

$$m_{\Xi_c(2815)^+} - m_{\Xi_c(2815)^0} = (-3.4 \pm 1.9(\text{stat}) \pm 0.9(\text{syst})) \text{ MeV}/c^2,$$

They are determined with a much better precision than the current world averages. The measurement also provides the first confirmation of the respective CLEO observations [12, 13].

In the $\Xi_c(2645)^+ \pi^-$ and $\Xi_c(2645)^0 \pi^+$ spectra, two states with masses around 2980 MeV/ c^2 are observed with large statistical significance. The measured masses and widths of the $\Xi_c(2980)$ are slightly different from the values determined for the $\Xi_c(2980)$ in previous measurements [1, 2], although still consistent within the uncertainties. While identification of this state as the $\Xi_c(2980)$ ([1, 2]) is plausible, further high-statistics measurements of its properties would be welcome to confirm this hypothesis.

TABLE V: Masses of the $\Xi_c(2645)$ and $\Xi_c(2815)$.

Particle	Mass [MeV/c ²]	
	PDG	This study
$\Xi_c(2645)^+$	2646.6 ± 1.4	$2645.6 \pm 0.2(\text{stat})_{-0.8}^{+0.6}(\text{syst})$
$\Xi_c(2645)^0$	2646.1 ± 1.2	$2645.7 \pm 0.2(\text{stat})_{-0.7}^{+0.6}(\text{syst})$
$\Xi_c(2815)^+$	2816.5 ± 1.2	$2817.0 \pm 1.2(\text{stat})_{-0.8}^{+0.7}(\text{syst})$
$\Xi_c(2815)^0$	2818.2 ± 2.1	$2820.4 \pm 1.4(\text{stat})_{-1.0}^{+0.9}(\text{syst})$

ACKNOWLEDGEMENTS

We thank the KEKB group for the excellent operation of the accelerator, the KEK cryogenics group for the efficient operation of the solenoid, and the KEK computer group and the National Institute of Informatics for valuable computing and Super-SINET network support. We acknowledge support from the Ministry of Education, Culture, Sports, Science, and Technology of Japan and the Japan Society for the Promotion of Science; the Australian Research Council and the Australian Department of Education, Science and Training; the National Natural Science Foundation of China under contract No. 10575109 and 10775142; the Department of Science and Technology of India; the BK21 program of the Ministry of Education of Korea, the CHEP SRC program and Basic Research program (grant No. R01-2005-000-10089-0) of the Korea Science and Engineering Foundation, and the Pure Basic Research Group program of the Korea Research Foundation; the Polish State Committee for Scientific Research; the Ministry of Education and Science of the Russian Federation and the Russian Federal Agency for Atomic Energy; the Slovenian Research Agency; the Swiss National Science Foundation; the National Science Council and the Ministry of Education of Taiwan; and the U.S. Department of Energy.

-
- [1] R. Chistov *et al.* (Belle Collaboration), *Phys. Rev. Lett.* **97**, 162001 (2006).
 - [2] B. Aubert *et al.* (BaBar Collaboration), *Phys. Rev. D* **77**, 012002 (2008).
 - [3] R. Mizuk *et al.* (Belle Collaboration), *Phys. Rev. Lett.* **98**, 262001 (2007).
 - [4] B. Aubert *et al.* (BaBar Collaboration), *Phys. Rev. D* **72**, 052006 (2006).
 - [5] B. Aubert *et al.* (BaBar Collaboration), *Phys. Rev. Lett.* **98**, 012001 (2007).
 - [6] B. Aubert *et al.* (BaBar Collaboration), *Phys. Rev. Lett.* **99**, 062001 (2007) and *Phys. Rev. Lett.* **97**, 232001 (2006).
 - [7] S.B. Athar *et al.* (CLEO Collaboration), *Phys. Rev. D* **71**, 051101 (2005).
 - [8] T. Lesiak *et al.* (Belle Collaboration), *Phys. Lett. B* **605**(2004) 237 and *Phys. Lett. B* **617** (2005) 198 (erratum).
 - [9] S. Capstick, N. Isgur, *Phys. Rev. D* **34**, 2809 (1986);
Yong-seok Oh, Byung-Yoon Park, *Phys. Rev. D*, **53**, 1605 (1996).
 - [10] N. Isgur, M.B. Wise, *Phys. Rev. Lett.* **66**, 1130 (1991).
 - [11] Charge-conjugate modes are implicitly included everywhere, unless specified otherwise.
 - [12] L. Gibbons *et al.* (CLEO Collaboration), *Phys. Rev. Lett.* **77**, 810 (1996).

- [13] J.P. Alexander *et al.* (CLEO Collaboration), *Phys. Rev. Lett.* **83**, 3390 (1999).
- [14] S. Kurokawa and E. Kikutani, *Nucl. Instr. Meth. A* **499**, 1 (2003), and other papers included in this Volume.
- [15] A. Abashian *et al.* (Belle Collaboration), *Nucl. Instr. Meth. A* **479**, 117 (2002).
- [16] R.E. Kalman, *Trans. Am. Soc. Mech. Eng. D.* **82**, 35 (1960);
R.E. Kalman and R.S. Bucy., *ibid.* **83**, 95 (1961).
- [17] The z -axis is oriented opposite to the direction of the e^+ beam, along the symmetry axis of the detector.
- [18] For protons attributed to the decay $\Lambda \rightarrow p\pi$, the hadron identification criterion was relaxed relative to the one described in the section “Track reconstruction and identification”.
- [19] n.d.f. denotes the number of degrees of freedom.
- [20] W.-M. Yao *et al.* *J. Phys. G*, **33**, 1 (2006) and 2007 partial update (URL: <http://pdg.lbl.gov/>).
- [21] S.E. Csorna *et al.* (CLEO Collaboration), *Phys. Rev. Lett.* **86**, 4243 (2001).
- [22] In the denominators of (6) and (7) we use $\epsilon(\Xi_c^{0,+})$ instead of $\epsilon(\Xi_c^{0,+}\pi^{+,-})$ as the charged pions are reconstructed and identified at Belle with a high overall efficiency, exceeding 80 %. As described in the text, this approximation is considered conservatively in the estimation of the systematic error.